ARTICLE
Journal of Cellular Biochemistry 108:555–564 (2009)

Journal of Cellular Biochemistry

Microtubule-Associated Protein Tau in Human Prostate Cancer Cells: Isoforms, Phosphorylation, and Interactions

Skye Souter and Gloria Lee*

Program in Molecular and Cellular Biology, Department of Internal Medicine, Roy J. and Lucille A. Carver College of Medicine, University of Iowa, Iowa City, Iowa 52242

ABSTRACT

Tau is a microtubule-associated protein whose function has been investigated primarily in neurons. Recently, tau expression has been correlated with increased drug resistance in various cancers of non-neuronal tissues. In this report, we investigate the tau expressed in cancerous prostate lines ALVA-31, DU 145, and PC-3. Prostate cancer tau is heat-stable and highly phosphorylated, containing many of the modifications identified in Alzheimer's disease brain tau. RT-PCR and phosphatase treatment indicated that all six alternatively spliced adult brain tau isoforms are expressed in ALVA-31 cells, and isoforms containing exon 6 as well as high molecular weight tau isoforms containing either exon 4A or a larger splice variant of exon 4A are also present. Consistent with its hyperphosphorylated state, a large proportion of ALVA-31 tau does not bind to microtubules, as detected by confocal microscopy and biochemical tests. Finally, endogenous ALVA-31 tau can interact with the p85 subunit of phosphatidylinositol 3-kinase, as demonstrated by co-immunoprecipitations and in vitro protein-binding assays. Our results suggest that tau in prostate cancer cells does not resemble that from normal adult brain and support the hypothesis that tau is a multifunctional protein. J. Cell. Biochem. 108: 555–564, 2009.

KEY WORDS: TAU; PROSTATE CANCER CELLS; MICROTUBULE BINDING; PHOSPHORYLATION; PHOSPHATIDYLINOSITOL 3-KINASE

Tau is a microtubule-associated protein (MAP) originally purified from brain and recognized for its ability to promote microtubule (MT) assembly in vitro [Weingarten et al., 1975]. Much interest in tau stems from its presence in the neurofibrillary tangles of Alzheimer's disease (AD) and other age-related neurodegenerative diseases, where it is abnormally phosphorylated [reviewed by Johnson and Stoothoff, 2004; Hernandez and Avila, 2007]. Since phosphorylation can reduce the affinity of tau for MTs, the inability of disease tau to carry out MT-related functions has been proposed as a major mechanism for AD pathogenesis [reviewed by Feinstein and Wilson, 2005].

A lesser known finding is that tau expression is not restricted to neurons; its presence has been demonstrated in several cell and tissue types including liver and skeletal muscle, among others [Kim et al., 1991; Ashman et al., 1992; Gu et al., 1996; Thurston et al., 1996; Vanier et al., 1998; Botez et al., 1999; Nagao et al., 1999; Cross et al., 2000]. In addition, a number of studies have drawn a connection between tau and drug resistance in non-neuronal cancers. Fellous and co-workers demonstrated that an estramustine-resistant prostate cancer line showed higher levels of tau than its drug-sensitive parental line [Sangrajrang et al., 1998]. More recently, a clinical study involving microarray analysis of a collection of breast cancer tissue samples identified tau as the single gene whose upregulation most consistently correlated with resistance to paclitaxel therapy [Rouzier et al., 2005], and a follow-up survey of breast cancer cell lines exhibited the same trend [Wagner et al., 2005]. Studies of gastric cancer tissue showed the same correlation between tau and paclitaxel resistance [Mimori et al., 2006] while a pancreatic cancer study showed a correlation between tau levels and resistance to different anti-mitotic compounds derived from benzoylphenylurea [Jimeno et al., 2007]. It has been proposed that the efficacy of MT targeting drugs in these cells had been compromised by tau due to tau's ability to compete with the drugs for MT-binding sites. However, in contrast to our knowledge of tau in normal and AD brain, little is known regarding the properties of tau in cancer cells. In this study, we set out to investigate tau in a

GenBank accession number FJ429137 (Homo sapiens high molecular weight microtubule-associated protein tau mRNA, exon 4A-L, and partial cds, alternatively spliced).

Additional Supporting Information may be found in the online version of this article.

Grant sponsor: National Cancer Institute (NCI); Grant number: CA103672; Grant sponsor: University of Iowa Cancer and Aging Program Research Development Funding Initiative; Grant number: NIH P20.

*Correspondence to: Dr. Gloria Lee, Department of Internal Medicine, Roy J. and Lucille A. Carver College of Medicine, University of Iowa, ML B191, 500 Newton Road, Iowa City, IA 52242. E-mail: gloria-lee@uiowa.edu

Received 27 May 2009; Accepted 25 June 2009 • DOI 10.1002/jcb.22287 • © 2009 Wiley-Liss, Inc.

Published online 13 August 2009 in Wiley InterScience (www.interscience.wiley.com).

cancer cell system. Our results shed new light on the expression and interactions of tau in non-neuronal cells and suggest that similarities exist between the tau found in age-related diseases such as prostate cancer and AD. Our data also suggest that the function of tau in prostate cancer cells may be distinct from that of tau in the normal adult brain.

MATERIALS AND METHODS

CELL CULTURE

Prostate cell lines 267B1, ALVA-NEO [Rokhlin et al., 1997], ALVA-hCD40 [Rokhlin et al., 1997], and DU 145 were obtained from Dr. Gail Bishop, LNCaP and PC-3 cells from Dr. Charles Yeaman, ALVA-31 from Dr. Michael Cohen, MCF7 breast cancer cells and U-2 OS osteosarcoma cells from Dr. Mary Horne, and PC6-3 rat pheochromocytoma cells from Dr. Henry Paulson. All prostate cells were grown in Opti-MEM containing 10% fetal bovine serum (FBS). PC6-3 cells were grown on 50 μg/ml collagen in RPMI 1640 with 5% FBS and 10% horse serum. SH-SY5Y cells and the stable derivative SH 9.13 expressing human 0N3R tau were grown as previously described [Lee et al., 1998; Sarkar et al., 2008]. MCF7 cells were grown in MEM with 10% FBS and 5 μg/ml bovine insulin. U-2 OS cells were grown in DMEM with 10% FBS. All media were supplemented with 2 mM L-glutamine, 100 U/ml penicillin G sodium, and 100 μg/ml streptomycin sulfate.

ANTIBODIES

Polyclonals CR and PY18, and monoclonal 9G3 were produced as previously described [Lee et al., 2004]. Monoclonals tau1 [Binder et al., 1985], tau-5 [LoPresti et al., 1995], tau-12 [Ghoshal et al., 2002], and tau-13 [Garcia-Sierra et al., 2003] were obtained from Dr. Lester Binder (Northwestern University), PHF-1 [Greenberg et al., 1992] and CP9 [Kohnken et al., 2000] from Dr. Peter Davies (Albert Einstein College of Medicine), 12E8 [Seubert et al., 1995] from Dr. Peter Seubert (Elan Pharmaceuticals), and JLA20 anti-actin from Dr. Jim Jung-Chin Lin (University of Iowa, through the Developmental Studies Hybridoma Bank; NICHD). Monoclonal AT8 [Mercken et al., 1992] was purchased from Pierce, tau14 from Zymed Laboratories, anti-PI3K p85 from BD Transduction Laboratories, and polyclonal anti-glutathione *S*-transferase (GST) from GE Healthcare. Purified mouse and rabbit IgGs, mouse IgG_{2a}, and monoclonal DMα1 anti-tubulin were purchased from Sigma, and monoclonal YL1/2 anti-tubulin from Harlan Sera-Lab/Accurate. Alexa488-conjugated goat anti-mouse IgG and Alexa594-conjugated phalloidin were purchased from Molecular Probes. Rhodamine Red-X donkey anti-rat IgG and horseradish peroxidase (HRP)-linked secondary antibodies (donkey anti-mouse IgG, goat anti-mouse IgM, and donkey anti-goat $F(ab')_2$ fragments) were purchased from Jackson Immunoresearch. HRP-linked goat anti-mouse IgG_1 (γ_1 chain specific) was purchased from SouthernBiotech.

IMMUNOPRECIPITATIONS

Cells (1 × 100 mm dish per reaction) were scraped into 1 ml pre-chilled Triton lysis buffer (1.0% Triton X-100, 0.25% deoxycholic acid, 50 mM Tris pH 7.5, 150 mM NaCl) containing protease and phosphatase inhibitors as previously described [Lee et al., 1998]. Following centrifugation (30 min at 7,700*g*, 4°C), the resulting supernatants were immunoprecipitated with either CR (5 μg/ml) or a combination of CR and PY18 (5 and 10 μg/ml, respectively) antisera; control immunoprecipitations were performed with 5 or 15 μg purified rabbit IgG. Immunoblots were probed with tau-12, tau-13, tau14, tau1, PHF-1, CP9, or 12E8.

For 9G3 immunoprecipitations, cells (1 × T150 flask per reaction) were lysed in 1 ml of Triton lysis buffer as described above. Lysates were pre-cleared with 4 μg purified mouse IgG_{2a} and protein A-sepharose (PAS; GE Healthcare) prior to immunoprecipitation with 4 μg of either 9G3 or control mouse IgG_{2a}. Immunoblots were probed with tau-12 and detected by IgG_1-specific HRP-coupled secondary to minimize detection of the 9G3 (an IgG_{2a}) used for immunoprecipitation.

For PI3K p85 co-immunoprecipitations, cells (4 × 150 mm dishes per reaction) were lysed in Triton/EDTA buffer (Triton lysis buffer described above supplemented with 1 mM EDTA, 1 mM EGTA, and 1 mM PMSF). Lysates were pre-cleared with 10 μg rabbit IgG or 3 μg mouse IgG_{2a} prior to immunoprecipitation with 10 μg CR or 3 μg anti-PI3K p85, respectively. Immunoblots were probed with either anti-PI3K p85 or tau-13. Tau-13 was detected by IgG_1-specific HRP-coupled secondary.

HEAT-STABLE PROTEIN PREPARATION

Cells (20–30 × 150 mm dishes per preparation) were scraped into pre-chilled MES buffer (20 mM MES pH 6.8, 750 mM NaCl, 2 mM DTT, 1 mM EGTA, 1 mM EDTA, inhibitors as described above), 1 ml per dish, and sonicated. Following centrifugation (20 min at 51,000*g*, 4°C) the resulting supernatants were boiled for 5 min, then chilled 10 min in ice water. Boiled lysates were cleared (20 min at 29,000*g*, 4°C), then dialyzed against 20 mM Tris pH 7.5, 1 mM PMSF. The resulting solution was concentrated and protein concentration was determined by Bradford method.

PCR AND RT-PCR REACTIONS

Total RNA was isolated from cells (2 × T150 flasks per preparation) using the RNAeasy Kit (Qiagen). First strand cDNA synthesis and first round PCR amplification were performed on 1.0 μg of RNA using the SuperScript III one-step RT-PCR system (Invitrogen) with primers 0 and Z, which amplify full-length *MAPT* mRNA; locations of all primers used are shown in Figures 2A and S1A, and primer sequences are listed in Figure S1B. First round cDNA synthesis was carried out at 55°C for 30 min followed by a 50 μl PCR reaction (40 cycles) with an annealing temperature of 55°C as outlined in manufacturer's instructions. Platinum Taq DNA polymerase (Invitrogen) was substituted for SuperScript III RT/Platinum Taq mix in no-RT control reactions. Second round PCR (30 cycles) was performed on 2 μl of the first round product in a 50 μl reaction containing 5 U of Taq polymerase in standard Taq buffer (New England Biolabs) using nested primer sets and an annealing temperature of 55°C. Pilot reactions using 35 or 40 cycles previously indicated that under our conditions, the product levels in the second round PCR reaction were below saturation at 30 cycles (data not shown). PCR products were resolved on 5% acrylamide/TBE gels.

DNA PURIFICATION AND SEQUENCING

PCR products of interest were eluted from polyacrylamide gels and purified with the QIAquick Gel Extraction kit (Qiagen).

All PCR products from reaction 2-D (Fig. 2B) were sequenced with reverse primer D, which allowed complete sequencing through all N-terminal exons present in each product. Products 0, 1, and 2 from reaction 1-B (Fig. 2B) were sequenced with forward primers 1, 2, and 3, respectively.

PHOSPHATASE TREATMENT

Up to 6.5 μg heat-stable protein was treated with 5 U CIAP (Roche) for 8 h at 37°C in a 20 μl reaction containing dephosphorylation buffer (Roche) and 1 M urea. Pilot experiments revealed completion of the reaction after less than 4 h of CIAP treatment with no additional gel mobility shifts observed between 4 and 24 h (data not shown). *Escherichia coli*-synthesized tau of each of the six human brain isoforms was used as a reference for dephosphorylated tau.

IMMUNOFLUORESCENCE

ALVA-NEO cells were grown on SonicSeal slides (Nunc) and glutaraldehyde-fixed as previously described [Lee and Rook, 1992]. Confocal microscopy was performed using a Nikon E600 microscope with a 60× oil immersion objective and Bio-Rad MRC-1024 system. Images were processed in Confocal Assistant, ImageJ, and Adobe Photoshop.

MICROTUBULE (MT)-BINDING ASSAYS

Triton X-100-soluble and -insoluble fractions were prepared from cells (1 × 100 mm dish per assay for ALVA-NEO and SH 9.13, 4 × 100 mm dishes per assay for PC6-3) in RAB buffer as previously described [Vogelsberg-Ragaglia et al., 2000]. Equal proportions of the soluble and insoluble fractions were resolved and immunoblotted with tau-12 or DMα1. Neuronal cell line PC6-3 was differentiated for 5 days with 100 ng/ml nerve growth factor (NGF) prior to harvesting.

Taxol-stabilized MTs were prepared as previously described [Vallee, 1986a]. Briefly, ALVA-NEO cells (12 × 150 mm dishes per preparation) were homogenized in pre-chilled PEM buffer. Following centrifugation (20 min at 24,000*g*, 4°C) and further fractionation (90 min at 136,000*g*, 4°C), the cleared supernatant was incubated with 1 mM GTP and 20 μM taxol (Calbiochem) at 37°C. After pelleting (45 min at 355,000*g*, 30°C), the resulting MT proteins were washed with 0.4 M KCl in PEM to remove MAPs [Vallee, 1986b]. Washed MTs were resuspended in PEM and protein concentration determined by Coomassie staining and densitometry against known standards.

Bovine brain MAPs were purified from a bovine brain MT protein preparation, generated as previously described [Vallee, 1986a]. The preparation was first treated with GTP and taxol as described above. After pelleting the MTs, MAPs were isolated by retaining the washes as described above. MAPs were desalted and concentration determined by Bradford method prior to use.

For MT-binding assays, 2 μg purified ALVA-NEO MTs was combined with either 0.2 μg 0N3R *E. coli* tau, 0.1 μg purified bovine MAPs, 20 μg heat-stable SH-SY5Y protein, 20 μg heat-stable ALVA-NEO protein, or no protein (MT only control) in a total volume of 60 μl containing 20 μM taxol and 1 mM GTP in PEM. Reactions were incubated at 37°C for 30 min. MTs were pelleted (45 min at 89,000*g*, 25°C), and equal proportions of the supernatant and pellet fractions were immunoblotted with either a tau cocktail of tau-13 and tau-5, or DMα1.

GST FUSION PROTEIN-BINDING ASSAYS

GST-PI3K p85-SH3 fusion protein was expressed in DH5α cells, affinity purified on glutathione sepharose, and quantified as previously described [Lee et al., 1998]. Confluent ALVA-NEO cells (3 × 150 mm dishes per assay) were lysed in 1 ml of Triton/EDTA buffer as described above. Binding assays were performed as previously described [Lee et al., 1998]. Assays were immunoblotted with tau-13 or anti-GST.

RESULTS

PROSTATE CANCER CELLS EXPRESS TAU

Tau has previously been described in the DU 145 prostate cancer cell line [Sangrajrang et al., 1998]. To extend these findings, we examined additional prostate cancer cell lines (ALVA-31, LNCaP, PC-3) and non-cancerous prostate epithelial cells (267B1). Substantial levels of tau protein were detected in ALVA-31 and DU 145 cells, and modest levels were found in PC-3 cells (Fig. 1A, left panel). Both low molecular weight and high molecular weight (HMW) forms of tau were found. LNCaP and 267B1 cells showed no significant tau expression even when the blot was deliberately overexposed (Fig. 1A, right panel). To address the possibility of heterogeneity in the cell lines, two clonal ALVA-31 derivatives [ALVA-NEO and ALVA-hCD40, Rokhlin et al., 1997] were also analyzed; both lines showed the same tau species as the parental line. We found similar protein patterns when we examined tau by immunoprecipitation (Fig. 1B). In comparison to the human neuroblastoma line SH-SY5Y, which expresses primarily the fetal tau isoform [Smith et al., 1995], prostate cancer cells showed a wider variety of tau species and comparable levels of total tau. As an additional criterion, we determined whether prostate cancer cells contain heat-stable tau, as heat stability is a characteristic property of neuronal tau [Weingarten et al., 1975]. The ALVA-NEO line was chosen for further analysis due to its clonality and high level of tau expression, and a heat-stable protein preparation from ALVA-NEO cells showed a tau pattern similar to that of the total cell lysate (Fig. 1C). We subsequently confirmed that ALVA-hCD40, DU 145, and PC-3 cells also contained heat-stable tau (data not shown).

PROSTATE CANCER CELLS EXPRESS MULTIPLE TAU ISOFORMS

The multiple tau species seen in prostate cancer cells may be due to alternative splicing. The *MAPT* gene encoding tau contains two alternatively spliced exons (exons 2 and 3) in the N-terminus and one (exon 10) in the C-terminus [Andreadis et al., 1992]. As exon 3 is never present in the absence of exon 2, the expression of six tau isoforms, termed 0N3R, 1N3R, 2N3R, 0N4R, 1N4R, and 2N4R, has been described in normal adult human brain [reviewed by Andreadis, 2005]. In the peripheral nervous system, HMW tau isoforms are also found; these contain exon 4A, which almost doubles the molecular weight of tau [Couchie et al., 1992; Goedert

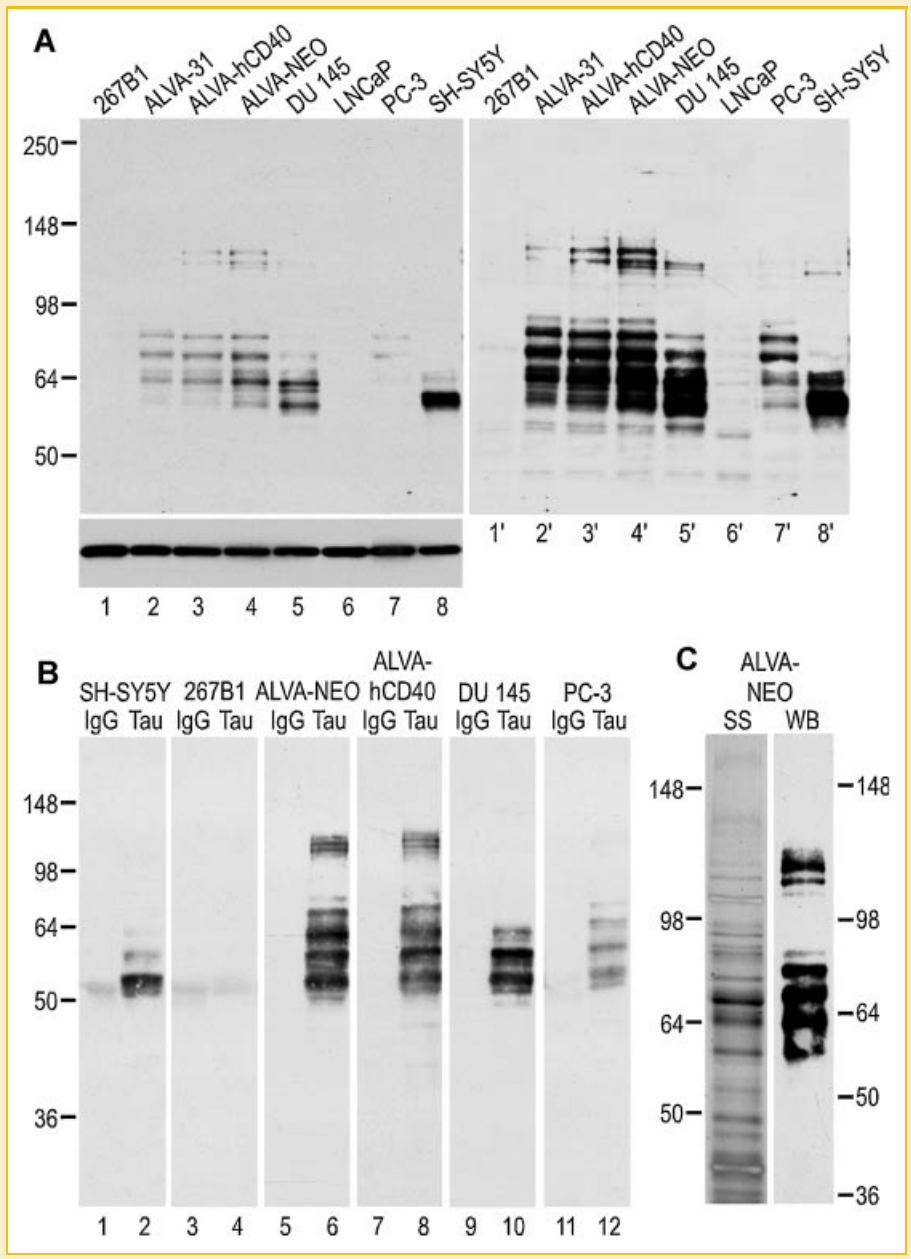

Fig. 1. Multiple forms of tau are expressed in prostate cancer cell lines. A: Cell lysates from the indicated cell lines were probed for total tau by immunoblotting with tau-13. Lanes 1′–8′ show a longer exposure of lanes 1–8. Tau was detected in the human prostate cancer lines DU 145, PC-3, ALVA-31, and in clonal ALVA-31 derivatives ALVA-NEO and ALVA-hCD40. The non-cancerous prostate line 267B1 (lane 1) and the cancerous line LNCaP (lane 6) showed no signal even after significant overexposure (lanes 1′ and 6′). SH-SY5Y human neuroblastoma cells were included for comparison. Actin served as a loading control (bottom panel). B: Tau was immunoprecipitated from prostate cancer cells using polyclonal anti-tau (even lanes) as described in the Materials and Methods Section; control immunoprecipitations used non-specific rabbit IgG (odd lanes). Immunoprecipitations were probed for total tau with tau-13. C: Heat-stable protein from ALVA-NEO cells was silver stained (SS) or probed for total tau with tau-13 (WB).

et al., 1992]. In addition, minor alternatively spliced exons such as exon 6 have been described, though their function is not completely understood [Andreadis et al., 1992; Luo et al., 2004].

To determine the isoforms that are expressed in the prostate cancer cells, we performed RT-PCR on total RNA from ALVA-NEO cells, followed by second round PCR using the primers outlined in Figures 2A and S1. Amplification of the N-terminal and C-terminal regions, in addition to amplification with primers specific to exons 2, 3, and 10, indicated that all six *MAPT* isoforms normally expressed in human brain are also expressed in ALVA-NEO cells. To determine if this *MAPT* expression pattern was specific to prostate cancer, we also examined MCF7 breast cancer cells, which have been previously reported to express tau [Rouzier et al., 2005]. We found nearly identical *MAPT* expression profiles in both cell types (Fig. S2A).

We also looked for the expression of exons 4A and 6. Amplification with primers specific to exon 4A confirmed its expression in combination with all three possible N-terminal splice

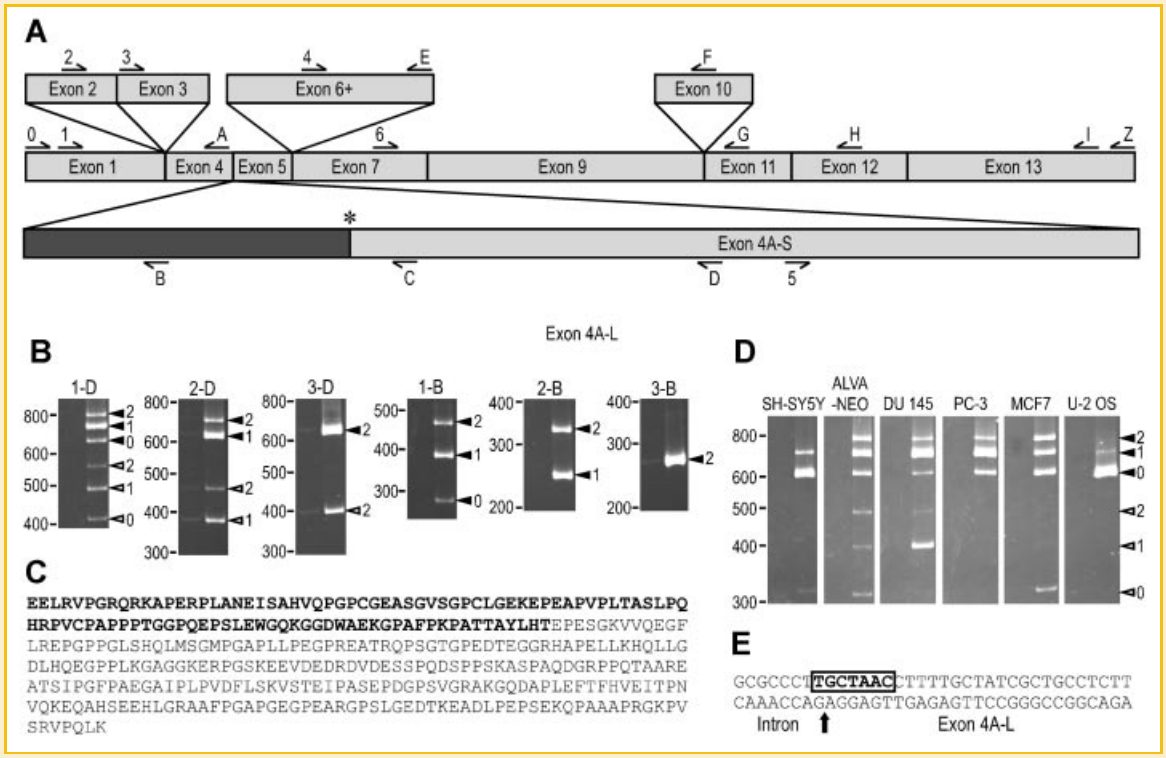

Fig. 2. ALVA-NEO cells express multiple tau isoforms, including a HMW variant not described in rodents. Total RNA from ALVA-NEO cells was reverse transcribed and PCR amplified as described in the Materials and Methods Section. A: To scale schematic of the *MAPT* coding sequence with the locations of PCR primers indicated. Numbered primers are forward primers, whereas lettered primers are reverse primers. Sequences of primers are given in Figure S1B. The large exon below, exon 4A-L, comprises exon 4A-S plus additional coding sequence (shaded) at the 5′ end of exon 4A. The asterisk marks the alternative splicing site within exon 4A-L that produces the HMW tau homologous to those proteins reported in mouse and rat. B: PCR products generated by exon-specific primers detecting high molecular weight *MAPT* isoforms. The primers used are indicated at the top of each panel; the left lane in each panel contains the no-RT control reaction. Products were run on 5% TBE–acrylamide gels. Several reactions yielded multiple bands, suggesting the presence of more than one *MAPT* isoform. Filled arrowheads indicate PCR products containing the shaded sequence shown in A; open arrowheads indicate PCR products lacking this sequence. To the right of the arrowheads, 0, 1, and 2 indicate products derived from 0N, 1N, and 2N tau isoforms. PCR products in the panels 1-B and 2-D were subjected to DNA sequencing. C: Predicted amino acid sequence of exon 4A-L. Bolded sequence corresponds to the new sequence contributed by the shaded sequence in (A). D: PCR products generated by exon-specific primers 1 and C, comparing the prevalence of exons 4A-S and 4A-L. Total RNA from seven human cell lines were reverse transcribed and PCR amplified as described in the Materials and Methods Section; filled arrowheads indicate PCR products containing exon 4A-L, while open arrowheads indicate products containing exon 4A-S. The left lane in each panel contains the no-RT control reaction. E: Genomic sequence surrounding the exon 4A-L 3′ splice site; the splice site is indicated by the arrow and the boxed boldface sequence indicates a potential branchpoint.

variants and both C-terminal variants (Fig. S2C). We obtained a similar result when amplifying with exon 6-specific primers (Fig. S2B). Of the three distinct splice variants of exon 6 that have been described (6+, 6p, and 6d) [Wei and Andreadis, 1998], the 6+ form appears to be the predominant form expressed in ALVA-NEO cells and its presence was confirmed by DNA sequencing (data not shown). The expression of exons 4A and 6 do not necessarily correlate with each other, although they can be seen together (Fig. S2B, panel 5-E). The sequencing data confirmed the presence of exon 4A in both the presence of and absence of exon 6+ in ALVA-NEO cells (data not shown).

While PCR reactions with the exon 4A-specific primers (1 and D) yielded products whose sizes matched those expected for the HMW tau cDNA from rat and mouse [Couchie et al., 1992; Goedert et al., 1992] (Figs. 2B and S2C, open arrowheads), the reactions also yielded similarly proportioned products about 300 bp longer (Figs. 2B and S2C, filled arrowheads). Sequencing of these PCR products revealed an additional 312 bp sequence inserted between exons 4 and 4A (Fig. 2A, shaded region). Because this sequence is adjacent to the 5′ end of exon 4A in the human genomic sequence, we will refer to this longer exon as "exon 4A-L" and the original exon 4A as "exon 4A-S." Exon 4A-L contains 1,065 bp, two 3′ splice sites, and encodes 355 aa (Fig. 2C). PCR with a primer specific to this additional sequence (Fig. 2A, primer B) revealed its presence in SH-SY5Y, DU 145, and PC-3 cells (data not shown). In addition, RT-PCR analysis of MCF7 cells and U-2 OS osteosarcoma cells suggested that inclusion of exon 4A-L is preferred over that of exon 4A-S in all human cells examined (Fig. 2D, primers 1 and C). These data indicate that the *MAPT* expression patterns described here are not limited to prostate cancer cells.

PROSTATE CANCER TAU IS HIGHLY PHOSPHORYLATED

To confirm the RT-PCR data at the protein level and to address the possibility of phosphorylation, we treated heat-stable tau preparations with alkaline phosphatase. It is well established that phosphorylation slows tau mobility, and that this mobility can be

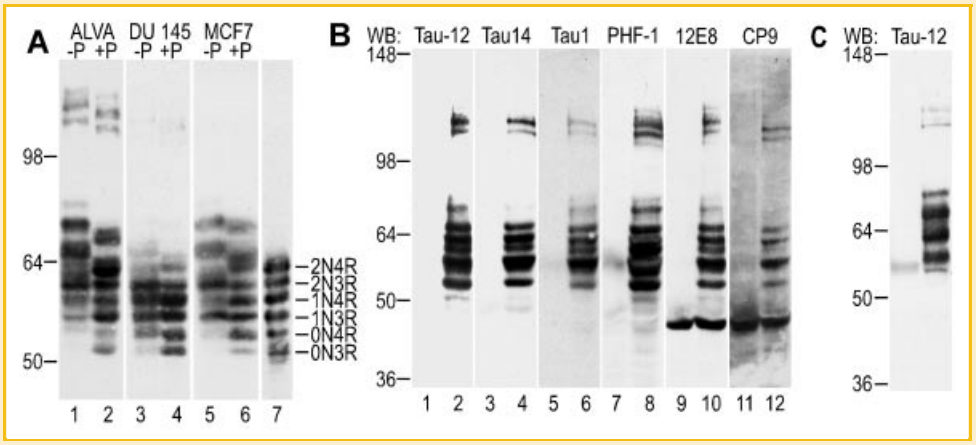

Fig. 3. ALVA-NEO tau is phosphorylated at multiple sites. A: Heat-stable protein from ALVA-NEO, DU 145, and MCF7 cells was incubated with alkaline phosphatase as described in the Materials and Methods Section (even lanes). Comparison with control incubations (odd lanes) indicated that phosphatase treatment increased the mobility of both high and low molecular weight tau. *E. coli*-synthesized tau proteins of each of the six major brain isoforms were run for comparison (lane 7). B: ALVA-NEO lysates were immunoprecipitated with polyclonal anti-tau as described in the Materials and Methods Section (even lanes); control immunoprecipitations used non-specific rabbit IgG (odd lanes). Immunoprecipitations were probed for total tau (lanes 1–4), or for specific tau phosphorylation states with the antibodies indicated (lanes 5–12). ALVA-NEO tau showed immunoreactivity with PHF-1 (phospho-Ser396/Ser404), 12E8 (phospho-Ser262/Ser356), CP9 (phospho-Thr231), and tau1 (non-phospho-Ser202/Ser205). C: ALVA-NEO lysate was immunoprecipitated with 9G3 (phospho-Tyr18) as described in the Materials and Methods Section (right lane); control immunoprecipitation used non-specific mouse IgG_{2a} (left lane). Immunoprecipitation was probed for total tau with tau-12.

altered by phosphatase treatment. Following phosphatase treatment, both HMW and low molecular weight forms of tau migrated faster, suggesting that both are phosphorylated (Fig. 3A, even lanes). However, multiple HMW and low molecular weight tau species were still present, confirming the RT-PCR findings. In fact, several of the lower molecular weight forms in phosphatase-treated ALVA-NEO, DU 145, and MCF7 tau co-migrated with specific *E. coli*-synthesized tau isoforms (Fig. 3A, lanes 2, 4, 6, and 7).

To examine specific phosphorylation sites in tau, we probed tau immunoprecipitations from ALVA-NEO cells with various phospho-specific antibodies [Binder et al., 1985; Otvos et al., 1994; Seubert et al., 1995; Kohnken et al., 2000]. ALVA-NEO tau showed phosphorylation at Ser396/Ser404, Ser262/Ser356, and Thr231 as detected by antibodies PHF-1, 12E8, and CP9, respectively (Fig. 3B, lanes 8, 10, and 12). Immunoprecipitation with the antibody 9G3 [Lee et al., 2004] showed that ALVA-NEO tau was phosphorylated at Tyr18 (Fig. 3C). Absence of phosphorylation at Ser202/Thr205 was detected by tau1 (Fig. 3B, lane 6); in agreement, we obtained no signal when probing with AT8, which detects phosphorylation at these sites (data not shown). Total tau was detected by tau-12 and tau14 (Fig. 3B, lanes 2 and 4). These findings were also confirmed by Western blotting in which ALVA-NEO heat-stable protein was probed with phospho-specific antibodies (data not shown).

NON-CYTOSKELETAL LOCALIZATION OF TAU

The localization of tau in cancer cells was examined using confocal microscopy. While tau co-localized with MTs at the cell periphery, there also appeared to be a significant population of free, unbound tau (Fig. 4). In mitotic cells, tau localized to the mitotic spindle, as previously reported [Preuss et al., 1995], but the presence of unbound tau was clearly evident. There was no apparent co-localization of tau with actin (data not shown).

To assess the proportion of prostate cancer tau that interacts with tubulin, we performed both Triton extractions and MT-binding assays. Triton extraction of ALVA-NEO cells revealed a large proportion of the tau in the Triton-soluble fraction (Fig. 5A, lane 1). Because polymerized MTs reside in the Triton-insoluble fraction, these data suggest that in ALVA-NEO cells, a majority of tau does not bind to the cytoskeleton. By comparison, in two neuronal cell lines, the tau appeared almost exclusively in the Triton-insoluble fraction (Fig. 5A, lanes 4 and 6).

The ability of ALVA-NEO tau to bind MTs in vitro was compared with that of purified *E. coli* 0N3R tau, SH-SY5Y tau, and bovine brain MAPs. To assure relevancy to the cancer cells, the assays were performed with MTs prepared from ALVA-NEO cells. While the *E. coli*, SH-SY5Y, and bovine brain MAPs bound to ALVA-NEO MTs (Fig. 5B, lanes 4, 6, and 8), much of the ALVA-NEO tau remained unbound (Fig. 5B, lane 1). An assay performed with twice the amount of ALVA-NEO tau resulted in a proportionate increase in bound and unbound proteins, indicating that the lack of binding was not due to a saturation of binding sites on the MTs (data not shown). These results indicate that the MT-binding affinity of ALVA-NEO tau is less than that of *E. coli* or neuronal tau.

ALVA-NEO TAU INTERACTS WITH PI3K

A recent report showed that in vitro, tau can interact with the SH3 domain of phosphatidylinositol 3-kinase (PI3K) [Reynolds et al., 2008], a multisubunit enzyme involved in Akt signaling. Because PI3K/Akt signaling is associated with cell survival and proliferation

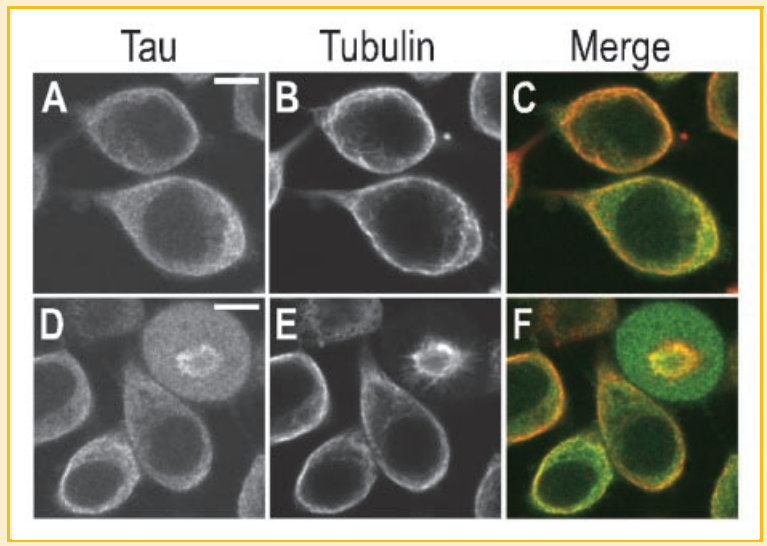

Fig. 4. Localization of tau in ALVA-NEO cells. Fixed ALVA-NEO cells were double-labeled with tau-12 (A,D) and YL1/2 anti-tubulin (B,E) and visualized by confocal microscopy. In interphase cells, tau appeared diffusely distributed throughout the cytoplasm; co-localization with tubulin occurred mainly in the cell periphery. In mitotic cells, tau was seen in the mitotic spindle as well as in the cytoplasm. Scale bar = 10 μm.

in many cancers, we investigated the interaction between tau and PI3K in prostate cancer cells. We found that tau immunoprecipitates contained the p85 regulatory subunit of PI3K and that p85 immunoprecipitates contained tau (Fig. 6A). Also, in a GST fusion protein-binding assay, ALVA-NEO tau bound to the SH3 domain of the p85 subunit of PI3K (Fig. 6B). Our results indicate that tau interacts with PI3K p85 in ALVA-NEO cells and implicate the SH3 domain in this interaction.

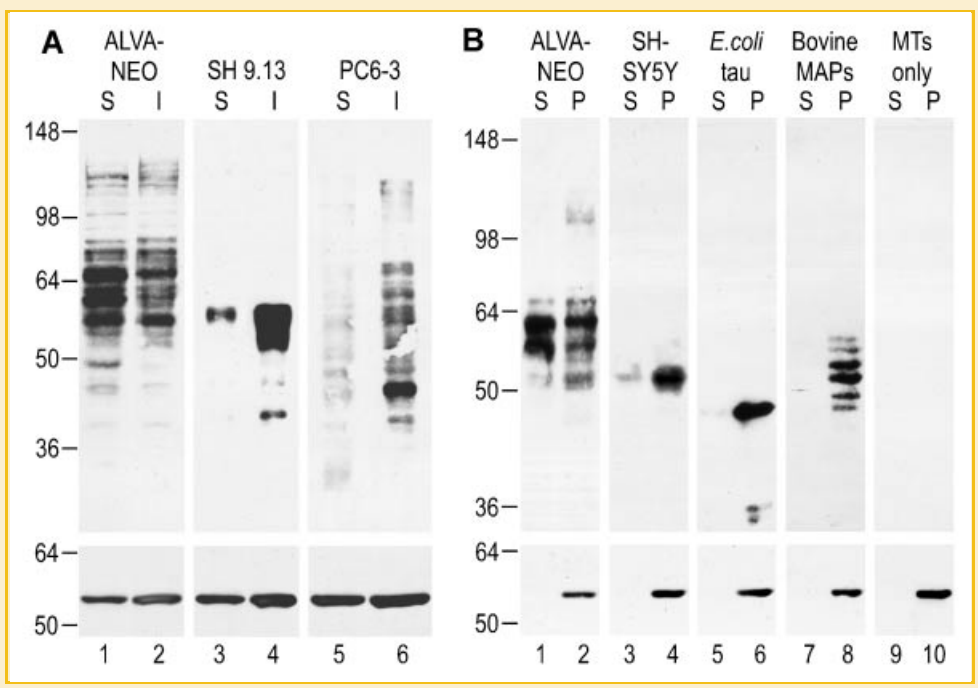

Fig. 5. A large pool of ALVA-NEO tau does not bind microtubules. A: ALVA-NEO, SH 9.13, and PC6-3 cells were subjected to 0.1% Triton X-100 extraction as described in the Materials and Methods Section. Equal proportions of the soluble (S; odd lanes) and insoluble (I; even lanes) fractions were probed for total tau with tau-13 or tau-5, and for tubulin with DMα1. Relative to the Triton-insoluble cytoskeletal fraction, ALVA-NEO cells show a larger proportion of tau in the Triton-soluble non-cytoskeletal fraction than SH 9.13 and PC6-3 cells. B: Heat-stable protein from ALVA-NEO and SH-SY5Y cells, *E. coli* tau, and bovine brain MAPs was incubated with ALVA-NEO microtubules as described in the Materials and Methods Section. Equal proportions of the supernatant (S; odd lanes) and the MT pellet (P; even lanes) were probed for total tau with tau-13 and tau-5, or for tubulin with DMα1. An MT only control was run to ensure that all endogenous tau was removed from the cancer cell MTs prior to the assay (lanes 9 and 10).

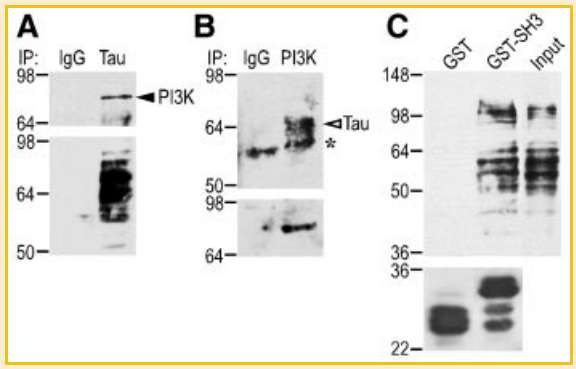

Fig. 6. ALVA-NEO tau interacts with PI3K. A: ALVA-NEO lysates were immunoprecipitated with polyclonal anti-tau (right lane) as described in the Materials and Methods Section; control immunoprecipitation used non-specific rabbit IgG (left lane). The immunoprecipitation was probed with either anti-PI3K p85 (top panel) or tau-13 to confirm immunoprecipitated tau (bottom panel). The co-immunoprecipitating PI3K is indicated by the filled arrowhead. B: ALVA-NEO lysates were immunoprecipitated with anti-PI3K p85 as described in the Materials and Methods Section; control immunoprecipitation used non-specific mouse IgG_{2a}. The resulting immunoprecipitation was probed with either tau-13 (top panel) or PI3K p85 to confirm immunoprecipitated PI3K (bottom panel). The co-immunoprecipitating tau is indicated by the open arrowhead. The asterisk indicates the IgG used for immunoprecipitation. C: ALVA-NEO lysates were incubated with either GST or GST-PI3K p85-SH3 as described in the Materials and Methods Section. The GST-bound proteins were probed for total tau with tau-13 (top panel). GST fusion proteins were probed with anti-GST (bottom panel).

DISCUSSION

Previous studies on non-neuronal tau have revealed novel properties of tau. Its tyrosine phosphorylation was first reported in monocytes [Kim et al., 1991], and its localization to the nucleus was described in HeLa cells, human lymphocytes, and human fibroblasts [Thurston et al., 1996]. Interest in non-neuronal tau has re-emerged stemming from clinical studies that have shown a correlation between tau levels and resistance to anti-mitotic drugs in various cancers [Rouzier et al., 2005; Mimori et al., 2006; Jimeno et al., 2007]. Our interest in tau from cancer cells was also motivated by the hypothesis that AD might be viewed as a cancer where a loss of cell-cycle control has occurred [reviewed by Yang and Herrup, 2007].

In this report, we have performed a comprehensive examination of tau expression in prostate cancer cells at both the mRNA and protein levels. The results indicate that cancerous prostate cells ALVA-31, DU 145, and PC-3 express high levels of tau, and that the complex pattern of tau seen is due to alternative splicing and phosphorylation. Given that many human and rodent neuronal cell lines as well as non-neuronal lines previously examined do not express multiple tau isoforms [Smith et al., 1995], the presence of all six brain isoforms in one cell line makes ALVA-31 a promising cell system to investigate adult human tau. The variability in tau expression levels that we noted across our panel was similarly observed in a survey of breast cancer cell lines [Rouzier et al., 2005; Wagner et al., 2005].

The expression of exon 4A-S and the presence of HMW tau species have been reported in several non-neuronal rat tissues [Gu et al., 1996]. However, in human, we also found a larger splice variant which we have termed exon 4A-L which produces exon 4A-S when a 3′ splice junction within exon 4A-L is utilized (Fig. 2A, asterisk); the expression of exon 4A-L has been previously reported in human skeletal muscle tissue [Wang et al., 2007]. In every human cell line we tested by RT-PCR, the 1,065 bp exon 4A-L appeared to be expressed in higher amounts than the 753 bp exon 4A-S (Fig. 2D). The exon 4A-L 3′ splice junction (CAG/A) matches the consensus sequence for splice sites, and examination of the upstream genomic sequence revealed a consensus branch point sequence (TGCTAAC) 35 bp upstream followed by a 28 bp pyrimidine-rich sequence (Fig. 2E). The presence of these elements, which favor splicing, may explain why exon 4A-L was the preferred splice product in the human cell lines examined, as exon 4A-S lacks both elements [Andreadis et al., 1992]. In addition, there is a stop codon encoded within the analogous 312 bp sequence in both mouse and rat (Fig. S3), and neither contains a consensus branchpoint sequence within 100 bp of the position analogous to the human branchpoint. Furthermore, even under the circumstances where an exon 4A-L splice junction in rodents would result in exclusion of these stop codons, the predicted protein sequence encoded by the mouse/rat 312 bp upstream of exon 4A-S shared only 17% identity with the corresponding protein sequence encoded by the human exon 4A-L sequence (Fig. 2C, boldface text), whereas 46% identity was shared by the protein sequences of rat, mouse, and human exon 4A-S. Thus, it is unlikely that the larger human HMW tau is expressed in rodent.

Our data indicate that human prostate cancer tau features phosphorylation normally absent in adult brain tau but present in neurodegenerative disease. Phospho-Thr231 has been found in AD brain and several other age-related neurodegenerative diseases [Husseman et al., 2000] and is an early marker for AD, appearing in pre-tangle tau [Augustinack et al., 2002]. Phospho-Ser396/Ser404 is present in both intra- and extracellular tangles in AD brain [Augustinack et al., 2002]; because this modification is upregulated during mitosis [Preuss et al., 1995], perhaps it is not surprising that cancer cell tau is modified in this manner. Phospho-Ser262/Ser356, also present in AD [Seubert et al., 1995], greatly reduces the MT-binding affinity of tau [Biernat et al., 1993], and its presence is consistent with our finding that a large pool of ALVA-NEO tau does not bind MTs in vitro and in vivo. Finally, phospho-Tyr18 is also present in both ALVA-NEO tau and in paired helical filaments and AD brain [Lee et al., 2004]. Of all the tau phosphorylation sites tested, phospho-Ser202/Thr205 was the only disease-related tau epitope that was absent, as indicated by the presence of tau1 immunoreactivity and the absence of AT8 immunoreactivity. While one might argue that AT8 might be generated by neuron-specific disease-related pathways, AT8 immunoreactivity has been found in the abnormal tau in diseased muscle cells of individuals with inclusion-body myositis [Mirabella et al., 1996]. These findings underline the complexity of the pathways that regulate tau phosphorylation.

In the studies that have shown a correlation between tau expression and drug resistance [Sangrajrang et al., 1998; Rouzier

et al., 2005; Wagner et al., 2005], a competition between tau and the drugs for binding sites on MTs was proposed to explain the relationship between tau and drug resistance. However, our finding that a large proportion of prostate cancer tau does not bind MTs suggests that other mechanisms should be considered. Moreover, irrespective of whether or not tau is able to compete with anti-mitotic drugs for MT-binding sites, the role of tau in cancer cells may not be primarily associated with MT assembly and binding, but rather with cell signaling.

Our results demonstrate the in vivo association of tau and the p85 subunit of PI3K, extending the in vitro binding data previously reported [Reynolds et al., 2008]. Because tau could not be co-immunoprecipitated with the p85 subunit of PI3K following overexpression in CHO cells [Reynolds et al., 2008], we speculate that the association takes place in prostate cancer cells because of the non-cytoskeletal characteristic of cancer cell tau. That is, since overexpressed tau in transfected cells is largely MT-associated, it may not associate with PI3K because of the proximity of the PI3K interaction site (aa 209–223) [Reynolds et al., 2008] to sites on tau involved in MT interaction [Mukrasch et al., 2007].

In view of the increasing number of similarities between cancer and AD and our finding that tau in cancer cells has similarities to tau in AD, one might consider the possibility that aging may activate similar pathways in both neuronal and non-neuronal cells. Neuronal and non-neuronal cells share many signaling components such as PI3K, MAPK, and mTOR. Further investigation of the tau in cancer cells may provide additional information about tau and cell-cycle regulation, which will be valuable to both the AD and cancer fields.

ACKNOWLEDGMENTS

We thank Drs. Gail Bishop, Michael Cohen, Mary Horne, Gail Johnson, Henry Paulson, and Charles Yeaman for cell lines, Drs. Lester Binder, Peter Davies, Dawn Quelle, Peter Seubert, and Jim Jung-Ching Lin for antibodies, Dr. Roland Brandt for the bovine brain protein preparation, and Dr. Hamid Band for the pGEX-PI3K-SH3 construct. We thank Dr. Athena Andreadis for the critical reading of the manuscript. We thank Drs. Frederick Domann, David Lubaroff, and Robert Wallace for their interest. This work was funded, in part, by an award from the University of Iowa Cancer and Aging Program Research Development Funding Initiative (NIH P20, CA103672, P.I. R.B. Wallace).

REFERENCES

Andreadis A. 2005. Tau gene alternative splicing: Expression patterns, regulation and modulation of function in normal brain and neurodegenerative diseases. Biochim Biophys Acta 1739:91–103.

Andreadis A, Brown WM, Kosik KS. 1992. Structure and novel exons of the human tau gene. Biochemistry 31:10626–10633.

Ashman JB, Hall ES, Eveleth J, Boekelheide K. 1992. Tau, the neuronal heat-stable microtubule-associated protein, is also present in the cross-linked microtubule network of the testicular spermatid manchette. Biol Reprod 46:120–129.

Augustinack JC, Schneider A, Mandelkow EM, Hyman BT. 2002. Specific tau phosphorylation sites correlate with severity of neuronal cytopathology in Alzheimer's disease. Acta Neuropathol 103:26–35.

Biernat J, Gustke N, Drewes G, Mandelkow EM, Mandelkow E. 1993. Phosphorylation of Ser262 strongly reduces binding of tau to microtubules: Distinction between PHF-like immunoreactivity and microtubule binding. Neuron 11:153–163.

Binder LI, Frankfurter A, Rebhun LI. 1985. The distribution of tau in the mammalian central nervous system. J Cell Biol 101:1371–1378.

Botez G, Probst A, Ipsen S, Tolnay M. 1999. Astrocytes expressing hyperphosphorylated tau protein without glial fibrillary tangles in argyrophilic grain disease. Acta Neuropathol 98:251–256.

Couchie D, Mavilia C, Georgieff IS, Liem RK, Shelanski ML, Nunez J. 1992. Primary structure of high molecular weight tau present in the peripheral nervous system. Proc Natl Acad Sci USA 89:4378–4381.

Cross DC, Munoz JP, Hernandez P, Maccioni RB. 2000. Nuclear and cytoplasmic tau proteins from human nonneuronal cells share common structural and functional features with brain tau. J Cell Biochem 78:305–317.

Feinstein SC, Wilson L. 2005. Inability of tau to properly regulate neuronal microtubule dynamics: A loss-of-function mechanism by which tau might mediate neuronal cell death. Biochim Biophys Acta 1739:268–279.

Garcia-Sierra F, Ghoshal N, Quinn B, Berry RW, Binder LI. 2003. Conformational changes and truncation of tau protein during tangle evolution in Alzheimer's disease. J Alzheimers Dis 5:65–77.

Ghoshal N, Garcia-Sierra F, Wuu J, Leurgans S, Bennett DA, Berry RW, Binder LI. 2002. Tau conformational changes correspond to impairments of episodic memory in mild cognitive impairment and Alzheimer's disease. Exp Neurol 177:475–493.

Goedert M, Spillantini MG, Crowther RA. 1992. Cloning of a big tau microtubule-associated protein characteristic of the peripheral nervous system. Proc Natl Acad Sci USA 89:1983–1987.

Greenberg SG, Davies P, Schein JD, Binder LI. 1992. Hydrofluoric acid-treated tau PHF proteins display the same biochemical properties as normal tau. J Biol Chem 267:564–569.

Gu Y, Oyama F, Ihara Y. 1996. Tau is widely expressed in rat tissues. J Neurochem 67:1235–1244.

Hernandez F, Avila J. 2007. Tauopathies. Cell Mol Life Sci 64:2219–2233.

Husseman JW, Nochlin D, Vincent I. 2000. Mitotic activation: A convergent mechanism for a cohort of neurodegenerative diseases. Neurobiol Aging 21:815–828.

Jimeno A, Hallur G, Chan A, Zhang X, Cusatis G, Chan F, Shah P, Chen R, Hamel E, Garrett-Mayer E, Khan S, Hidalgo M. 2007. Development of two novel benzoylphenylurea sulfur analogues and evidence that the microtubule-associated protein tau is predictive of their activity in pancreatic cancer. Mol Cancer Ther 6:1509–1516.

Johnson GV, Stoothoff WH. 2004. Tau phosphorylation in neuronal cell function and dysfunction. J Cell Sci 117:5721–5729.

Kim H, Strong TV, Anderson SJ. 1991. Evidence for tau expression in cells of monocyte lineage and its in vitro phosphorylation by v-fms kinase. Oncogene 6:1085–1087.

Kohnken R, Buerger K, Zinkowski R, Miller C, Kerkman D, DeBernardis J, Shen J, Moller HJ, Davies P, Hampel H. 2000. Detection of tau phosphorylated at threonine 231 in cerebrospinal fluid of Alzheimer's disease patients. Neurosci Lett 287:187–190.

Lee G, Rook SL. 1992. Expression of tau protein in non-neuronal cells: Microtubule binding and stabilization. J Cell Sci 102(Pt 2):227–237.

Lee G, Newman ST, Gard DL, Band H, Panchamoorthy G. 1998. Tau interacts with src-family non-receptor tyrosine kinases. J Cell Sci 111(Pt 21):3167–3177.

Lee G, Thangavel R, Sharma VM, Litersky JM, Bhaskar K, Fang SM, Do LH, Andreadis A, Van Hoesen G, Ksiezak-Reding H. 2004. Phosphorylation of tau by fyn: Implications for Alzheimer's disease. J Neurosci 24:2304–2312.

LoPresti P, Szuchet S, Papasozomenos SC, Zinkowski RP, Binder LI. 1995. Functional implications for the microtubule-associated protein tau: Localization in oligodendrocytes. Proc Natl Acad Sci USA 92:10369–10373.

Luo MH, Leski ML, Andreadis A. 2004. Tau isoforms which contain the domain encoded by exon 6 and their role in neurite elongation. J Cell Biochem 91:880–895.

Mercken M, Vandermeeren M, Lubke U, Six J, Boons J, Van de Voorde A, Martin JJ, Gheuens J. 1992. Monoclonal antibodies with selective specificity for Alzheimer Tau are directed against phosphatase-sensitive epitopes. Acta Neuropathol 84:265–272.

Mimori K, Sadanaga N, Yoshikawa Y, Ishikawa K, Hashimoto M, Tanaka F, Sasaki A, Inoue H, Sugimachi K, Mori M. 2006. Reduced tau expression in gastric cancer can identify candidates for successful Paclitaxel treatment. Br J Cancer 94:1894–1897.

Mirabella M, Alvarez RB, Bilak M, Engel WK, Askanas V. 1996. Difference in expression of phosphorylated tau epitopes between sporadic inclusion-body myositis and hereditary inclusion-body myopathies. J Neuropathol Exp Neurol 55:774–786.

Mukrasch MD, von Bergen M, Biernat J, Fischer D, Griesinger C, Mandelkow E, Zweckstetter M. 2007. The "jaws" of the tau-microtubule interaction. J Biol Chem 282:12230–12239.

Nagao SI, Kumamoto T, Masuda T, Ueyama H, Toyoshima I, Tsuda T. 1999. Tau expression in denervated rat muscles. Muscle Nerve 22:61–70.

Otvos L, Jr., Feiner L, Lang E, Szendrei GI, Goedert M, Lee VM. 1994. Monoclonal antibody PHF-1 recognizes tau protein phosphorylated at serine residues 396 and 404. J Neurosci Res 39:669–673.

Preuss U, Doring F, Illenberger S, Mandelkow EM. 1995. Cell cycle-dependent phosphorylation and microtubule binding of tau protein stably transfected into Chinese hamster ovary cells. Mol Biol Cell 6:1397–1410.

Reynolds CH, Garwood CJ, Wray S, Price C, Kellie S, Perera T, Zvelebil M, Yang A, Sheppard PW, Varndell IM, Hanger DP, Anderton BH. 2008. Phosphorylation regulates tau interactions with Src homology 3 domains of phosphatidylinositol 3-kinase, phospholipase Cgamma1, Grb2, and Src family kinases. J Biol Chem 283:18177–18186.

Rokhlin OW, Bishop GA, Hostager BS, Waldschmidt TJ, Sidorenko SP, Pavloff N, Kiefer MC, Umansky SR, Glover RA, Cohen MB. 1997. Fas-mediated apoptosis in human prostatic carcinoma cell lines. Cancer Res 57:1758–1768.

Rouzier R, Rajan R, Wagner P, Hess KR, Gold DL, Stec J, Ayers M, Ross JS, Zhang P, Buchholz TA, Kuerer H, Green M, Arun B, Hortobagyi GN, Symmans WF, Pusztai L. 2005. Microtubule-associated protein tau: A marker of paclitaxel sensitivity in breast cancer. Proc Natl Acad Sci USA 102:8315–8320.

Sangrajrang S, Denoulet P, Millot G, Tatoud R, Podgorniak MP, Tew KD, Calvo F, Fellous A. 1998. Estramustine resistance correlates with tau over-expression in human prostatic carcinoma cells. Int J Cancer 77:626–631.

Sarkar M, Kuret J, Lee G. 2008. Two motifs within the tau microtubule-binding domain mediate its association with the hsc70 molecular chaperone. J Neurosci Res 86:2763–2773.

Seubert P, Mawal-Dewan M, Barbour R, Jakes R, Goedert M, Johnson GV, Litersky JM, Schenk D, Lieberburg I, Trojanowski JQ, Lee VM. 1995. Detection of phosphorylated Ser262 in fetal tau, adult tau, and paired helical filament tau. J Biol Chem 270: 18917–18922.

Smith CJ, Anderton BH, Davis DR, Gallo JM. 1995. Tau isoform expression and phosphorylation state during differentiation of cultured neuronal cells. FEBS Lett 375:243–248.

Thurston VC, Zinkowski RP, Binder LI. 1996. Tau as a nucleolar protein in human nonneural cells in vitro and in vivo. Chromosoma 105:20–30.

Vallee RB. 1986a. Purification of brain microtubules and microtubule-associated protein 1 using taxol. Methods Enzymol 134:104–115.

Vallee RB. 1986b. Reversible assembly purification of microtubules without assembly-promoting agents and further purification of tubulin, microtubule-associated proteins, and MAP fragments. Methods Enzymol 134:89–104.

Vanier MT, Neuville P, Michalik L, Launay JF. 1998. Expression of specific tau exons in normal and tumoral pancreatic acinar cells. J Cell Sci 111(Pt 10): 1419–1432.

Vogelsberg-Ragaglia V, Bruce J, Richter-Landsberg C, Zhang B, Hong M, Trojanowski JQ, Lee VM. 2000. Distinct FTDP-17 missense mutations in tau produce tau aggregates and other pathological phenotypes in transfected CHO cells. Mol Biol Cell 11:4093–4104.

Wagner P, Wang B, Clark E, Lee H, Rouzier R, Pusztai L. 2005. Microtubule associated protein (MAP)-tau: A novel mediator of paclitaxel sensitivity in vitro and in vivo. Cell Cycle 4:1149–1152.

Wang J, Tse SW, Andreadis A. 2007. Tau exon 6 is regulated by an intricate interplay of trans factors and cis elements, including multiple branch points. J Neurochem 100:437–445.

Wei ML, Andreadis A. 1998. Splicing of a regulated exon reveals additional complexity in the axonal microtubule-associated protein tau. J Neurochem 70:1346–1356.

Weingarten MD, Lockwood AH, Hwo SY, Kirschner MW. 1975. A protein factor essential for microtubule assembly. Proc Natl Acad Sci USA 72:1858–1862.

Yang Y, Herrup K. 2007. Cell division in the CNS: Protective response or lethal event in post-mitotic neurons? Biochim Biophys Acta 1772:457–466.